Experimental Mechanics (2009) 49:25–33
DOI 10.1007/s11340-007-9093-1

Changes in Intracellular Calcium during Compression of C2C12 Myotubes

K.K. Ceelen · C.W.J. Oomens · A. Stekelenburg · D.L. Bader · F.P.T. Baaijens

Received: 30 March 2007 / Accepted: 4 October 2007 / Published online: 10 November 2007

Abstract In recent years, damage directly due to tissue deformation has gained interest in deep pressure ulcer aetiology research. It has been shown that deformation causes muscle cell damage, though the pathway is unclear. Mechanically induced skeletal muscle damage has often been associated with an increased intracellular Ca^{2+} concentration, e.g. in eccentric exercise (Allen et al., J Physiol 567(3):723–735, 2005). Therefore, the hypothesis was that compression leads to membrane disruptions, causing an increased Ca^{2+}-influx, eventually leading to Ca^{2+} overload and cell death. Monolayers of differentiated C2C12 myocytes, stained with a calcium-sensitive probe (fluo-4), were individually subjected to compression while monitoring the fluo-4 intensity. Approximately 50% of the cells exhibited brief calcium transients in response to compression, while the rest did not react. However, all cells demonstrated a prolonged Ca^{2+} up-regulation upon necrosis, which induced similar up-regulations in some of the surrounding cells. Population heterogeneity is a possible explanation for the observed differences in response, and it might also become important in tissue damage development. It did not become clear however whether Ca^{2+}-influxes were the initiators of damage.

K.K. Ceelen (✉) · C.W.J. Oomens · A. Stekelenburg · D.L. Bader · F.P.T. Baaijens
Department of Biomedical Engineering, Eindhoven University of Technology, P.O. Box 513, 5600 MB Eindhoven, The Netherlands
e-mail: k.k.ceelen@tue.nl

D.L. Bader
Department of Engineering and IRC in Biomedical Materials, Queen Mary University of London, London, UK

Keywords Pressure ulcers · Aetiology · Deformation · Injury · Skeletal muscle

Introduction

Pressure ulcers are localized areas of degenerated soft tissue that develop due to prolonged mechanical loading. These ulcers can either originate in the skin surface, or within the deeper muscle layers adjacent to bony prominences. The latter so called deep pressure ulcers, involve deep tissue injury under an intact skin [1].

The precise damage mechanisms responsible for the development of these wounds are still unclear. Deformation-induced blood vessel collapse resulting in ischaemia may cause damage [2–4], and reperfusion upon tissue unloading can also be harmful [5, 6]. Fridén et al. [7] and Stekelenburg et al. [8] showed that compression and ischaemia together have a more damaging effect on muscle tissue than ischaemia alone.

Experiments on single cells by Bouten et al. [9] and on tissue-engineered muscle constructs by Breuls et al. [10] demonstrated that deformation itself affects cell viability. Gawlitta et al. [11] investigated the separate contributions of different aspects of compression to damage in an *in vitro* set-up. They found that deformation was, in the short term, more damaging to the cells than hypoxia. In addition, Stekelenburg et al. [12] showed that regions of damage in muscle tissues in an animal model corresponded to areas of maximum shear strain in indentation tests. These findings all indicate that tissue deformation per se leads to damage, and hence may be an important factor in damage development in deep pressure ulcers.

However, the temporal pathway from muscle deformation to gross tissue damage still remains unclear. It might be suggested that elevated intracellular Ca^{2+} levels are involved in the initiation of deep pressure ulcers, in a similar manner to that in skeletal muscle damage. Indeed, in eccentric contraction-induced injury, it is believed that membrane stretch leads to an increased membrane permeability, permitting an influx of Ca^{2+} ions [13, 14]. The mechanical destruction of muscle plasma membrane, and the passive stretching of muscle cells induced similar increases in intracellular Ca^{2+} [15–18].

The similarity in histological damage patterns from muscle indentation experiments on rats [12] and eccentric exercise-induced damage [19], further supports the idea of stretch-induced Ca^{2+}-influx and subsequent fibre injury in pressure-induced skeletal muscle injury. Furthermore, it is known that degrees of hypoxia and ischaemia induce an increase in intracellular Ca^{2+} in their damage pathways [20, 21]. Moens et al. [22] proposed that the ischaemic Ca^{2+} increase for cardiomyocytes involved a disturbed ion homeostasis starting with acidosis due to anaerobic metabolism. Fredsted et al. [20] found that the increased Ca^{2+} content induced by anoxia was associated with a loss of membrane integrity, further increasing Ca^{2+}-influx.

The present study tests the hypothesis that deformation leads to an increased Ca^{2+}-influx in a similar manner to ischaemia, although the specific mechanisms may be uncoupled. The cellular homeostatic processes are eventually compromised beyond which a cascade of events will lead to cell death.

To test the hypothesis, the following questions were addressed in the present study. Is cell death due to compression indeed preceded by an increase in intracellular Ca^{2+} concentration? Is there a certain compression threshold for mechanical cell damage? In order to examine this hypothesis, a well-defined *in vitro* muscle cell model subjected to deformation was stained with both a Ca^{2+}-sensitive dye and an indicator of cell necrosis. Fluorescence of these dyes was monitored while single myotubes were compressed to reveal the Ca^{2+} dynamics in response to cell compression.

Materials & Methods

Cell Culture

C2C12 murine skeletal myoblasts (ECACC, Salisbury, UK) were cultured in growth medium (GM) in an incubator at 37°C and 5% CO_2. GM consisted of 500 ml Dulbecco's modified Eagle's medium (DMEM) high glucose with L-glutamine (Gibco, The Netherlands), 15% FBS, 2% HEPES, 1% non-essential amino acids and 0.5% gentamicin (all from Biochrom AG, Germany). Between passages 13 and 17, cells were harvested and seeded in monolayers on gelatin-coated cover glasses placed in 6-well plates at a density of 75,000 to 100,000 cells/well. After 2 days, they were differentiated into myotubes with differentiation medium (DM) having the same formulation as GM, except that FBS was replaced by 2% horse serum (Biochrom AG).

Compression experiments were performed on differentiation day 4, a time at which myotubes were shown to be optimal in a pilot study.

Staining

The monolayers were stained with cell-permeant fluo-4 AM (F14201, Molecular Probes) to visualize cytosolic Ca^{2+} [18, 23], and cell tracker orange CMTMR (CTO, C2927, Molecular Probes) to visualize the cells. Fluo-4 was dissolved in DMSO to a concentration of 1 mM, and subsequently diluted in DMEM to a final concentration of 10 μM. This was supplemented with 5 μM CTO, and cells were incubated for 25 min. Thereafter, they were washed twice with DMEM and then incubated a further 15 min to ensure complete cleavage of fluo-4 by intracellular ester enzymes to release the Ca^{2+}-sensitive probe. This was performed in DM, supplemented with 10 μM propidium iodide (PI, P3566, Molecular Probes) to monitor necrosis [24]. Thereafter, the monolayer was transferred to the experimental set-up with 1 ml DM and a covering layer of mineral oil to prevent medium evaporation.

Mechanical Deformation

A custom-built cell compression device for unconfined compression of single attached cells designed in the host laboratory was employed [25]. It consists of a stainless steel frame resting on a motorized stage of an inverted microscope. A cover glass with cells was inserted in a polycarbonate cell chamber, where temperature and CO_2 were controlled. Cells were compressed using a glass indenter having a flat surface with a diameter of 50 μm. This indenter can be moved with three micromanipulators within a range of 15 mm at minimum increments of 50 nm. Fine-positioning was achieved with piezo-actuators within a range of 100 μm with a resolution of 5 nm.

Using a 40× magnification objective (Plan-Apochromat 40×/0.95 corr), one or two myotubes were selected for compression. The thickness of these myotubes was determined from a stack of confocal

Table 1 Overview of experiments

Series	Exp	# cells	t (inc-scan) (min)	Final deformation (%)
a	1	1 / 3	150	55
	2	2 / 3	360	70/63*
	3	1 / 5	150	55
	4	1 / 2	420	54
	5	2 / 4	90	54
b	6	1 / 5	120	78
	7	1 / 6	120	71
	8	2 / 9	50	50
c	9	0 / 12	105	0
	10	0 / 10	60	0

* The variation in compression levels can be attributed to the differences in height between the 2 cells.
# cells: number of compressed cells / total number of monitored cells.
t(inc-scan): time between fluo-4 incubation and scanning.

images of the CTO-stained myotube. From a stack of line scans, the height of the indenter above the cover glass could be estimated. The indenter was then moved using the micromanipulators to within 10 μm of the top of the myotube to be compressed. Then the piezo-actuators were used to apply deformation in increments of 1 μm. After the loading experiment, the indenter was further moved downwards in increments of 1 μm until slight contact was made with the cover glass, indicated by the force transducer. This determined the height of the indenter more accurately and enabled an estimation of the applied compression levels.

Two different compression regimes were used. In the first set of experiments, increments of 1 μm compression were applied until necrosis of the compressed myotube (series *a*), a process associated with an extended scanning period. By contrast, in the second set of experiments, larger increments of 2 to 3 μm were applied (series *b*). Control experiments were conducted in an identical experimental set-up in the absence of compression (series *c*). An overview of the experiments that have been performed is given in Table 1.

Data Acquisition and Analysis

The intensities of fluo-4, CTO and PI fluorescence were monitored on an inverted microscope (Axiovert 100 M, Zeiss, Germany) with a confocal laser scanning unit (LSM 510, Zeiss, Germany) using a 40× magnification objective. The three probes were excited with a 25 mW Argon laser at 488 nm. For detection of fluo-4 fluorescence, emission was recorded between 505 and 530 nm. Both CTO and PI fluorescence emission was measured above 585 nm. PI could be distinguished from CTO because the former predominantly stains the nuclei, and this fluorescence was much more intense than CTO fluorescence.

Time series consisted of images with a field of view of 230.3×230.3 μm^2 (512×512 pixels), a scanning time of 1 s and with no delay between two consecutive images.

Data were analyzed using MATLAB. Each compressed myotube was divided into several regions of interest (ROIs), corresponding to sections of the myotube that were either directly subjected to compression or not (Fig. 1). Other myotubes, which remained uncompressed, acted as controls. In the regions of interest, intensities of the red (CTO and PI) and green (fluo-4) channels were normalized to their respective intensities in the first frame. Only relative changes in fluo-4 intensity were studied since fluo-4 is not a ratiometric dye. This means that Ca^{2+}-independent spatial and temporal variations in intensity are superimposed on Ca^{2+}-dependent changes, which makes accurate calibration hardly feasible [23].

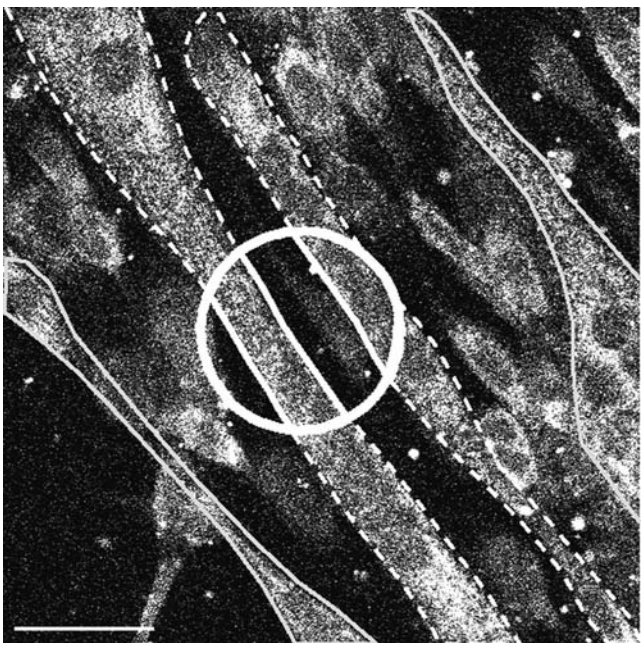

Fig. 1 CTO image with selected regions of interest: The white circle indicates the position of the indenter, solid white lines indicate ROIs under the indenter, ROIs surrounded by dashed white lines are parts of compressed tubes that are not under the indenter, and grey lines outline tubes that are not compressed. (*scale bar* 50 μm)

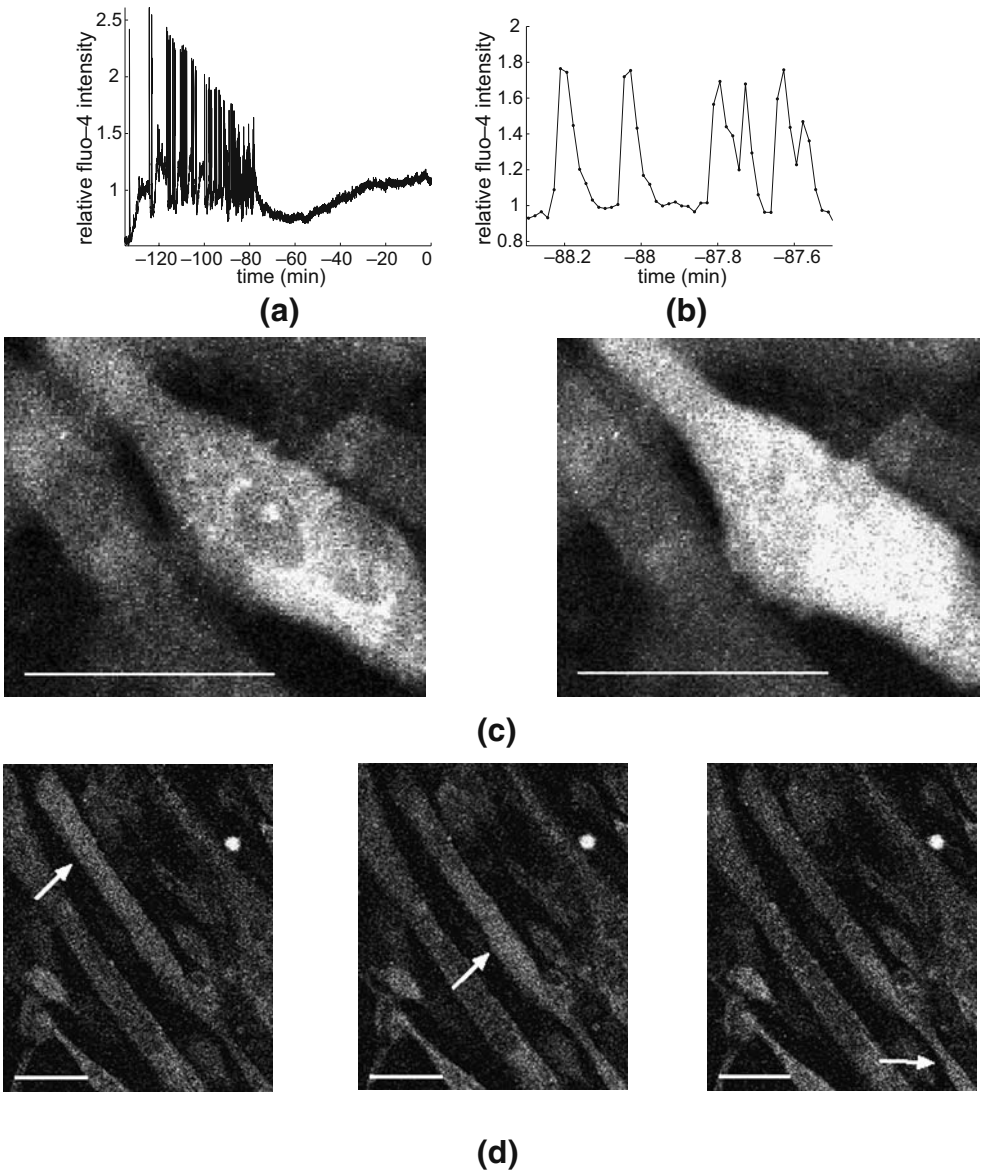

Fig. 2 (**a**, **b**) Temporal profiles of fluo-4 intensity, exhibiting oscillations with a decreasing amplitude at two different time scales. All data points are 1 s apart. (**c**) Two consecutive fluo-4 images showing a clear increase in fluo-4 intensity. (*scale bars* 50 μm) (**d**) Three consecutive fluo-4 images demonstrating that transients may start at one end of the myotube (*left arrow*) and then travel to the other end (*right arrow*). (*scale bars* 50 μm)

Results

Three aspects of the fluo-4 intensity were studied, i.e. baseline fluo-4 intensity, fluo-4 transients and fluo-4 up-regulations upon cell death. There was no systematic pattern in baseline fluo-4 intensity either before or during compression. Indeed, cells exhibited either no change, a decrease or an increase in fluo-4 intensity. However, at the point of cell death, a prolonged fluo-4 up-regulation was evident, lasting tens of seconds. Elevations in intracellular Ca^{2+} prior to cell death were much shorter, and they will be termed transients [Fig. 2(a)–(c)]. The frequency and amplitude of these transients varied from oscillating, high amplitude transients to isolated, low-amplitude transients. The difference between up-regulations and transients is illustrated in Fig. 3, showing transients occurring superimposed on a prolonged up-regulation of fluo-4 intensity.

Oscillatory Fluo-4 Transients

In all the experiments where the time between incubation of fluo-4 and scanning time series was less than or equal to 2 h, at least one cell exhibited a strongly fluctuating fluo-4 intensity. The oscillations were observed in both myoblasts and fused cells with more than one nucleus, although never in cells under compression. All increases in fluo-4 intensity occurred throughout the whole cell, although, in some cases, they started at one

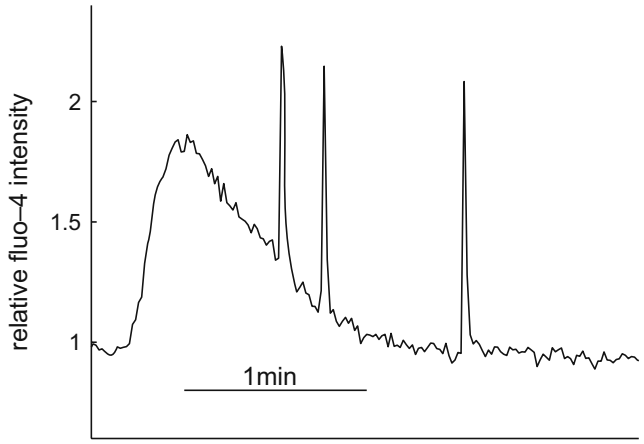

Fig. 3 Prolonged fluo-4 up-regulation and transients: An up-regulation in fluo-4 intensity, lasting for more than 1 min, is superimposed by fluo-4 transients, lasting only a few seconds

end of the cell and then traveled to the other end, as illustrated in Fig. 2(d).

The frequency of the transients varied from only 1 or 2 transients per hour to 2 to 3 transients per minute. Individual transients lasted up to a few seconds [Fig. 2(b)]. The peak intensity of the transients varied between 1.5 and 3 times the base intensity but in most cases the amplitude gradually declined and the oscillations stopped after 20 to 50 min [Fig. 2(a)].

Fluo-4 Transients During Compression

Based on the response during compression, cells were divided into 2 categories. One category included cells in which the fluo-4 intensity increased with an increment of compression, while the other category included cells that did not respond to the increments. Their different features are illustrated in Fig. 4. In both categories, however, a wide up-regulation of fluo-4 intensity accompanied the influx of PI. Of the 11 cells that were compressed, 5 could be characterized in category 1 (2 from series *a* and 3 from series *b*) and 6 in category 2 (5 from series *a* and 1 from series *b*).

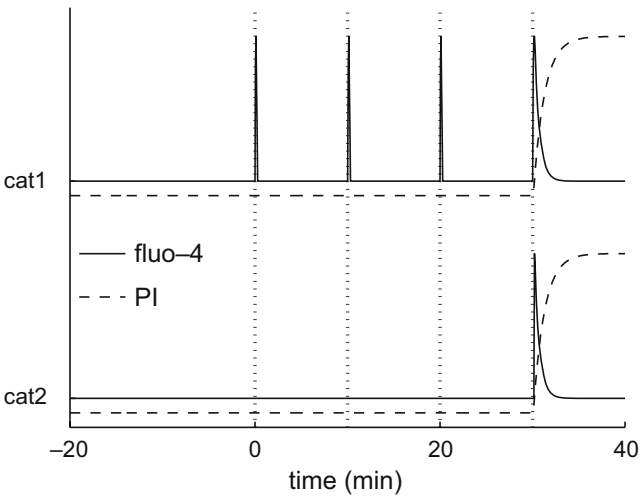

Fig. 4 Schematic representation of fluo-4 and PI intensities in 2 categories: In category 1 (*cat1*), fluo-4 intensity shows transients after an increment in compression (*vertical dotted lines*), and a wide up-regulation when PI enters the cell. In category 2 (*cat2*), fluo-4 intensity peaks when PI enters the cell, but there is no response to previous compression increments

Category 1: Compression-induced fluo-4 transients

In category 1, the fluo-4 intensity showed a transient shortly after an increment in compression. It is evident from the individual cell profiles in Fig. 5 that transients started to occur at a compression level of approximately 30%. In most of the experiments there were also transients before compression started, and in some there were transients during compression that were not directly associated with an increment in compression.

Category 2: Unresponsive fluo-4 intensity

Cells in category 2 did not show transients clearly associated with compression increments (Fig. 6). Some of these cells seemed very quiescent, exhibiting either no fluo-4 transients or only a few at low amplitude. Other cells did exhibit distinct fluo-4 transients, although these were not associated with a change in compression level.

Fluo-4 Up-regulations at Cell Death

When PI entered the nuclei, reflecting a necrotic state, fluo-4 intensity was up-regulated for an extended period. The profile was characterized by a steep rise and a much slower decline, amounting to a total duration of the up-regulation of the order of tens of seconds. Ten of the 11 cells that died exhibited this behavior although not necessarily in ROIs directly under the indenter. In all cases, the PI-influx occurred within 2 min of the onset of the Ca^{2+}-influx.

In 80% of cases, these fluo-4 up-regulations were accompanied by increases in fluo-4 intensity in at least one of the surrounding cells. Figure 7 depicts the temporal profiles of fluo-4 intensity in all selected cells of experiment 8 as an example of this interaction. However, not all the surrounding cells always participated in this intercellular Ca^{2+} wave, and the nature of this Ca^{2+} activity could not be correlated with either the actual distance from the compressed cell or the pattern of previous Ca^{2+} fluxes. The delay between the up-regulations in the dying cells and those in the

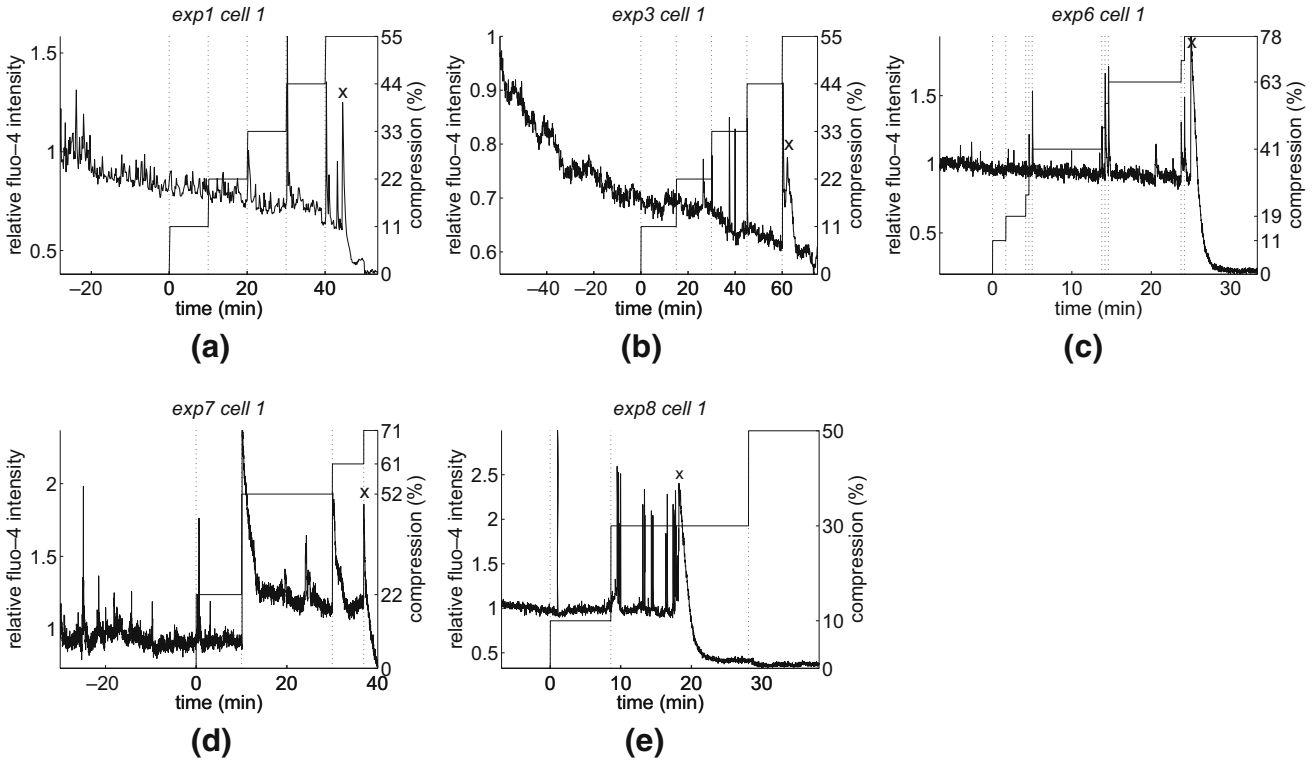

Fig. 5 Category 1: Temporal profiles of fluo-4 intensities (*left y-axes*) and compression levels (*right y-axes*) in compressed myotubes from experiments 1 (**a**), 3 (**b**), 6 (**c**), 7 (**d**) and 8 (**e**): This category is characterized by fluo-4 transients closely associated with increments in compression (indicated by vertical dotted lines). Wide fluo-4 up-regulations are visible when the cells die (indicated with a cross). Note that scales differ

surrounding cells was generally less than 15 s. There were no recurrent differences in either amplitude or duration between the up-regulations in the dying cells and those in the surrounding cells.

Discussion

In recent years, skeletal muscle cell damage directly due to tissue deformation has gained interest in the study of deep pressure ulcer aetiology. Mechanically induced skeletal muscle damage has often been associated with increased intracellular Ca^{2+} concentrations [13–18]. For example in Duchenne muscular dystrophy, muscle contraction leads to frequent occurrence of membrane disruptions. The resulting increased Ca^{2+}-influx gradually becomes lethally high [26–28].

In the present study, it was hypothesized that mechanical deformation makes the cell membrane more permeable, resulting in a Ca^{2+}-influx. The cell might accommodate for this influx by activating associated ion pumps to remove the Ca^{2+} ions from the cell or, at least, remove them to the sarcoplasmic reticulum. It might also be proposed that at some time point saturation of these mechanisms would result in Ca^{2+} overload. It is known that high Ca^{2+} concentrations activate calpains and phospholipase A2, and influence mitochondrial functioning, increasing the production of reactive oxygen species [29]. These effects make a Ca^{2+} overload a potentially harmful condition. However, the current data does not support the hypothesis. Indeed, increments of compression induced short Ca^{2+} transients in approximately half of the cells, while no response was observed in the other cells. In all cells, cell death was accompanied by a wide fluo-4 up-regulation, which often induced up-regulations in surrounding, viable cells.

Differentiated C2C12 cells in monolayers were used for the compression experiments. Monolayers were used instead of more realistic 3D bio-artificial muscle constructs [30] because precise levels of cell compression are difficult to determine and control within the 3D gel constructs. The incremental increase in compression used in the current study allows the possibility of determining a compression threshold for cell damage. A small deformation may only lead to adaptations in the C2C12 differentiation process [31], and the extent of stretch can influence the Ca^{2+} accumulation [17].

Liao et al. [18] incubated rat neonatal cardiomyocytes with fluo-4, and subjected them to 90 min of 20% passive stretch. This elicited high amplitude transients

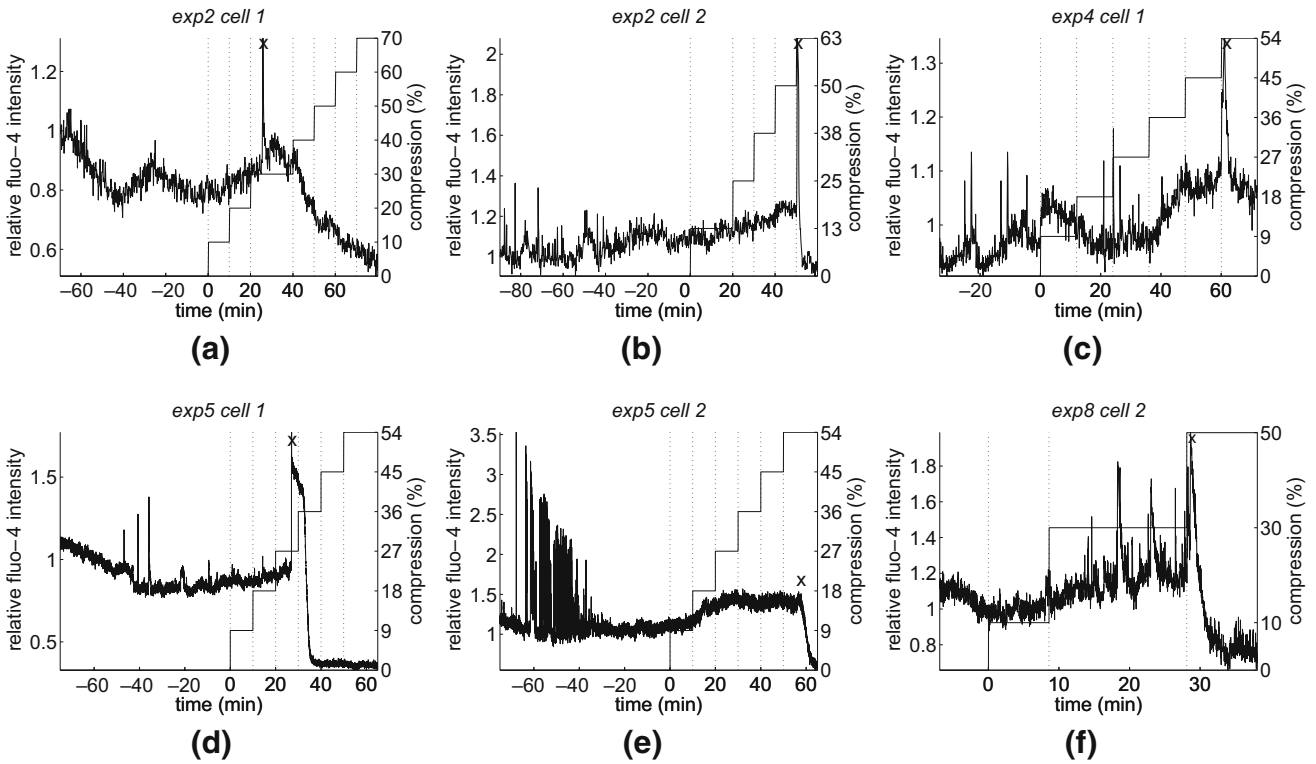

Fig. 6 Category 2: Temporal profiles of fluo-4 intensities (*left y-axes*) and compression levels (*right y-axes*) in compressed myotubes from experiments 2 (**a**+**b**), 4 (**c**), 5 (**d**+**e**), and 8 (**f**): This category is characterized by a lack of response of the fluo-4 intensity to changes in compression (indicated by vertical dotted lines). Wide fluo-4 up-regulations are visible when the cells die (indicated with a cross). Note that scales differ

that disappeared during the first 10 min of stretch, and a stable elevation of intracellular Ca^{2+} that persisted. After 4 h of 20% stretch, the number of apoptotic cells had significantly increased compared to the control situation. However, blocking of the stretch-induced Ca^{2+} elevation prevented apoptosis. A prolonged increase in intracellular Ca^{2+} was not observed in the current study. This might be due to a difference in response between cardiomyocytes and skeletal myocytes.

Hence, no damage threshold could be defined that marks the transition to gradual damage accumulation due to compression. Instead, the occurrence of fluo-4 transients could be used to determine a damage threshold. Cells that exhibited a transient in response to a compression increment, did this only when the compression level was at least 30%. At the point of cell death, there was always a wide Ca^{2+} up-regulation, inducing Ca^{2+} up-regulations in some of the surrounding cells as well. Considering the short time between this Ca^{2+}-influx and the PI-influx (Fig. 7), and the similar Ca^{2+} up-regulations in surviving cells, it is unlikely that this Ca^{2+}-influx is the cause of cell death.

The spread of the wide up-regulations before cell death was also seen by Kerkweg and De Groot [15] when they lethally destroyed the cell membrane of one myotube in a monolayer. Indeed this mechanically elicited intercellular Ca^{2+} wave is a well-known phenomenon in a variety of cells [32–35]. For example, in C2C12 murine skeletal muscle cells in a monolayer, its propagation results from liberation of ATP from the

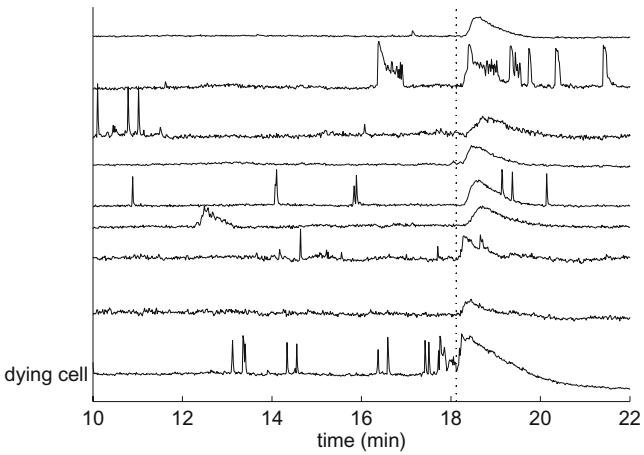

Fig. 7 Temporal profiles of fluo-4 intensity in 9 tubes that were selected in experiment 8: When the cell represented by the lowest trace died (indicated by the vertical dashed line), the fluo-4 up-regulation in this cell is accompanied by fluo-4 up-regulations in all other cells. There is a small delay between the up-regulation in the dying cell and the other cells, and a longer rise time in the latter

mechanically injured cell [15]. However, what exactly initiates the release of ATP is unclear. It would be interesting to examine what the initiator of the Ca^{2+} wave is, and what inhibition of this pathway would do to the cells that are involved.

Not all cells in the proximity of the compressed cells participated in the intercellular Ca^{2+} wave. Distance from the stimulated cell or previous Ca^{2+} dynamics cannot explain this. Differences in differentiation state of the cells might play a role. Lorenzon et al. [36] characterized Ca^{2+} transients in C2C12 cells during their differentiation. Both mononucleated cells and myotubes displayed relatively long Ca^{2+} transients of a few seconds, starting from day 3 in DM. On differentiation day 4, global spikes started to occur in a small proportion of cells [36]. These spikes occur in bursts of up to tens of minutes with varying frequency, interspersed with inactive periods as long as tens of minutes, a pattern that resembles the pattern of the oscillations in the present study. Differences in the occurrence of transients may be due to different developmental stages of the cells. Cseri et al. [37] observed that amplitude and kinetics of ATP-evoked Ca^{2+} transients also depended on the stage of development of the myotubes. Heterogeneity of the cell population might thus explain the observed behavior [38]. In addition, the time between fluo-4 incubation and scanning [39], and fatigue of Ca^{2+} receptors [40] could be important.

In summary, passive deformation of differentiated C2C12 murine skeletal muscle cells caused brief Ca^{2+} transients in approximately half of the cells, and no response in the other half. This difference might be explained by population heterogeneity, which might also be important in the development of tissue damage. Eventually cells became necrotic, which was accompanied by an increase in intracellular Ca^{2+}. The wide Ca^{2+} up-regulations in these dying cells induced similar up-regulations in some of the surrounding, viable cells. Ca^{2+} chelators, Ca^{2+} channel blockers and differentiation markers might reveal some differences between cells. They might also clarify whether Ca^{2+} transients and up-regulations are a prerequisite of cell death or just a side effect of cell degeneration.

Acknowledgement The authors would like to thank M.L.P. Langelaan for her helpful contributions to the experimental design and for performing pilot experiments.

References

1. Donnelly J (2005) Should we include deep tissue injury in pressure ulcer staging systems? The NPUAP debate. J Wound Care 14(5):207–210.
2. Daniel RK, Priest DL, Wheatley DC (1981) Etiologic factors in pressure sores: an experimental model. Arch Phys Med Rehabil 62:492–498.
3. Dinsdale SM (1974) Decubitus ulcers: role of pressure and friction in causation. Arch Phys Med Rehabil 55:147–152.
4. Kosiak M (1961) Etiology of decubitus ulcers. Arch Phys Med Rehabil 42:19–29.
5. Appell HJ, Gloser S, Soares JMC, Duarte JA (1999) Structural alterations of skeletal muscle induced by ischemia and reperfusion. Basic Appl Myol 9(5):263–268.
6. Blaisdell FW (2002) The pathophysiology of skeletal muscle ischemia and the reperfusion syndrome: a review. Cardiovasc Surg 10(6):620–630.
7. Fridén J, Pedowitz RA, Thornell LE (1994) Sensitivity of different types of fibres in rabbit skeletal muscle to pneumatic compression by tourniquet and to ischaemia. Scand J Plast Reconstr Surg Hand Surg 28:87–94.
8. Stekelenburg A, Strijkers GJ, Parusel H, Bader DL, Nicolay K, Oomens CWJ (2007) The role of ischemia and deformation in the onset of compression-induced deep tissue injury: MRI-based studies in a rat model. J Appl Physiol 102(5):2002–2011
9. Bouten CVC, Knight MM, Lee DA, Bader DL (2001) Compressive deformation and damage of muscle cell subpopulations in a model system. Ann Biomed Eng 29:153–163.
10. Breuls RGM, Bouten CVC, Oomens CWJ, Bader DL, Baaijens FPT (2003) Compression induced cell damage in engineered muscle tissue: an *in vitro* model to study pressure ulcer aetiology. Ann Biomed Eng 31:1357–1364.
11. Gawlitta D, Li W, Oomens CWJ, Baaijens FPT, Bader DL, Bouten CVC (2007) The relative contributions of compression and hypoxia to development of muscle tissue damage: an *in vitro* study. Ann Biomed Eng 35(2):273–284.
12. Stekelenburg A, Oomens CWJ, Strijkers GJ, Nicolay K, Bader DL (2006) Compression-induced deep tissue injury examined with magnetic resonance imaging and histology. J Appl Physiol 100(6):1946–1954.
13. Allen DG, Whitehead NP, Yeung EW (2005) Mechanisms of stretch-induced muscle damage in normal and dystrophic muscle: role of ionic changes. J Physiol 567(3):723–735.
14. Proske U, Morgan DL (2001) Muscle damage from eccentric exercise: mechanism, mechanical signs, adaptation and clinical applications. J Physiol 537(2):333–345.
15. Kerkweg U, De Groot H (2005) ATP-induced calcium increase as a potential first signal in mechanical tissue trauma. A laser scanning microscopic study on cultured mouse skeletal myocytes. Shock 24(5):440–446.
16. Armstrong RB, Duan C, Delp MD, Hayes DA, Glenn GM, Allen GD (1993) Elevations in rat soleus muscle [Ca^{2+}] with passive stretch. J Appl Physiol 74(6):2990–2997.
17. Ruwhof C, Van Wamel JET, Noordzij LAW, Aydin S, Harper JCR, Van der Laarse A (2001) Mechanical stress stimulates phospholipase C activity and intracellular calcium ion levels in neonatal rat cardiomyocytes. Cell Calcium 29(2):73–83.
18. Liao XD, Tang AH, Chen Q, Jin HJ, Wu CH, Chen LY, Wang SQ (2003) Role of Ca^{2+} signaling in initaition of stretch-induced apoptosis in neonatal heart cells. Biochem Biophys Res Commun 310:405–411.
19. Fridén J, Lieber RL (1998) Segmental muscle fiber lesions after repetitive eccentric contractions. Cell Tissue Res 293: 165–171.
20. Fredsted A, Mikkelsen UR, Gissel H, Clausen T (2005) Anoxia induces Ca^{2+} influx and loss of cell membrane integrity in rat extensor digitorum longus muscle. Exp Physiol 90(5):703–714.

21. Tóth A, Ivanics T, Ruttner Z, Slaaf DW, Reneman RS, Ligeti L (1998) Quantitative assessment of $[Ca^{2+}]_i$ levels in rat skeletal muscle in vivo. Am J Physiol Heart Circ Physiol 44:H1652–H1662.
22. Moens AL, Claeys MJ, Timmermans JP, Vrints CJ (2005) Myocaridal ischemia/reperfusion injury, a clinical view on a complex pathophysiological process. Int J Cardiol 100: 179–190.
23. Gee KR, Brown KA, Chen WNU, Bishop-Stewart J, Gray D, Johnson I (2000) Chemical and physiological characterization of fluo-4 Ca^{2+}-indicator dyes. Cell Calcium 27(2): 97–106.
24. Gawlitta D, Oomens CWJ, Baaijens FPT, Bouten CVC (2004) Evaluation of a continuous quantification method of apoptosis and necrosis in tissue cultures. Cytotechnology 46:139–150.
25. Peeters EAG, Bouten CVC, Oomens CVC, Baaijens FPT (2003) Monitoring the biomechanical response of individual cells under compression: a new compression device. Med Biol Eng Comput 41:498–503.
26. Alderton JM, Steinhardt RA (2000) How calcium influx through calcium leak channels is responsible for the elevated levels of calcium-dependent proteolysis in dystrophic myotubes. Trends Cardiovasc Med 10:268–272.
27. McNeil PL, Steinhardt RA (1997) Loss, restoration, and maintenance of plasma membrane integrity. J Cell Biol 137(1):1–4.
28. Deconinck N, Dan B (2007) Pathophysiology of Duchenne muscular dystrophy: current hypotheses. Pediatr Neurol 36(1):1–7.
29. Gissel H (2005) The role of Ca^{2+} in muscle cell damage. Ann N Y Acad Sci 1066:166–180.
30. Gawlitta D (2007) Compression-induced factors influencing the damage of engineered skeletal muscle. Ph.D. thesis, Eindhoven University of Technology.
31. Rauch C, Loughna PT (2006) Cyclosporin-A inhibits stretch-induced changes in myosin heavy chain expression in C2C12 skeletal muscle cells. Cell Biochem Funct 24:55–61.
32. Young RC, Schumann R, Zhang P (2002) The signaling mechanisms of long distance intercellular calcium waves (far waves) in cultured human uterine myocytes. J Muscle Res Cell Motil 23(4):279–284.
33. Suadicani SO, Vink MJ, Spray DC (2000) Slow intercellular Ca^{2+} signaling in wild-type and Cx43-null neonatal mouse cardiac myocytes. Am J Physiol Heart Circ Physiol 279:H3076–H3088.
34. Grandolfo M, Calabrese A, D'Andrea P (1998) Mechanism of mechnically induced intercellular calcium waves in rabbit articular chondrocytes and in HIG-82 synovial cells. J Bone Miner Res 13(3):443–453.
35. Arcuino G, Lin JHC, Takano T, Liu C, Jiang L, Gao Q, Kang J, Nedergaard N (2002) Intercellular calcium signaling mediated by point-source burst release of ATP. Proc Natl Acad Sci U S A 99(15):9840–9845.
36. Lorenzon P, Giovannelli A, Ragozzino D, Eusebi F, Ruzzier F (1997) Spontaneous and repetitive calcium transients in C2C12 mouse myotubes during *in vitro* myogenesis. Eur J Neurosci 9:800–808.
37. Cseri J, Szappanos H, Szigeti GP, Csernátony Z, Kovács L, Csernoch L (2002) A purinergic signal transduction pathway in mammalian skeletal muscle cells in culture. Pflügers Arch 443:731–738.
38. Pingguan-Murphy B, Lee DA, Bader DL, Knight MM (2005) Activation of chondrocytes calcium signalling by dynamic compression is independent of number of cycles. Arch Biochem Biophys 444:45–51.
39. Knight MM, Roberts SR, Lee DA, Bader DL (2003) Live cell imaging using confocal microscopy induces intracellular calcium transients and cell death. Am J Physiol Cell Physiol 284:C1083–C1089.
40. Allen DG, Westerblad H (2001) Role of phosphate and calcium stores in muscle fatigue. J Physiol 536(3): 657–665.